

**Dominant effects of organic carbon chemistry on decomposition dynamics of crop  
residues in a Mollisol**

Yehong Xu <sup>a, b</sup>, Zengming Chen <sup>a, b</sup>, Sébastien Fontaine <sup>c</sup>, Weijin Wang <sup>d, e</sup>, Jiafa Luo <sup>f</sup>,  
Jianling Fan <sup>a</sup>, Weixin Ding <sup>a, \*</sup>

<sup>a</sup> *State Key Laboratory of Soil and Sustainable Agriculture, Institute of Soil Science, Chinese  
Academy of Sciences, Nanjing 210008, China*

<sup>b</sup> *University of Chinese Academy of Sciences, Beijing 100049, China*

<sup>c</sup> *INRA, UR 874, Grassland Ecosystem Research Team, Clermont-Ferrand, France*

<sup>d</sup> *Department of Science, Information Technology and Innovation (DSITI), Dutton Park, QLD  
4102, Australia*

<sup>e</sup> *Environmental Futures Research Institute, Griffith University, Nathan, QLD 4111, Australia*

<sup>f</sup> *AgResearch Limited, Ruakura Research Centre, Hamilton 3240, New Zealand*

\* Corresponding author. Institute of Soil Science, Chinese Academy of Sciences, Nanjing  
210008, China. Tel.: +86 25 8688 1527. Fax: + 86 25 8688 1000.

*E-mail address:* wxding@issas.ac.cn (W. Ding)

## Abstract

Understanding the change in chemical composition of crop residues during their decomposition is crucial to elucidate the mechanisms underlying the effects of residue retention on soil carbon (C) sequestration and nutrient cycling. Here a field experiment was carried out to investigate the decomposition process of maize, soybean, and wheat residues in a cultivated Mollisol in northeast China over a year. Using a litterbag method, we monitored the dynamics of residue mass loss, concentration of C and nitrogen (N), and C/N ratio, and evaluated the decomposition rates of residues and C functional groups. Chemical compositions of the crop residues were determined by solid-state  $^{13}\text{C}$ -nuclear magnetic resonance spectroscopy, and the cellulose crystallinity, lignin concentration, and syringyl to guaiacyl (S/G) ratio of lignin were estimated. After one year of incubation in field conditions, mass loss was 57% for soybean residues, significantly greater than 52% for maize and 45% for wheat. The decomposition rate of residues significantly decreased from 0.223–0.379  $\text{month}^{-1}$  during the first month to 0.054–0.076  $\text{month}^{-1}$  over the whole period. The proportion of decomposed C ranged at 57–63% among different residues, and had a positive relationship with the mass loss of O-alkyl C, di-O-alkyl C, and carbonyl C. The decomposition rates of these three C functional groups were greater in soybean than those in maize and wheat residues, which was also the case for lignin S/G ratio, possibly accounting for the higher decomposition extent of soybean residues. As decomposition progressed, the C chemistry of maize, soybean, and wheat residues exhibited an increasing divergence, which was mainly related to relative decreases in O-alkyl C and di-O-alkyl C contents, and relative increases in

phenolic C and aromatic C contents in the residues. Net N release was observed for all residues after one-year decomposition, and was significantly related to the mass loss of alkyl C, O-alkyl C, and aromatic C. Overall, our study provides insight into chemical changes of crop residues over the degradation processes in the field, and highlights the significant effects of organic C chemistry on residue decomposition.

*Key words:* Crop residues; Litterbag; C decomposition; N release; Solid-state  $^{13}\text{C}$ -NMR

## 1. Introduction

The global soil organic carbon (SOC) storage is estimated at 1502 Pg in the upper meter of soil, more than 10% of which is stored in croplands (Jobbágy and Jackson, 2000). Enhancing SOC sequestration in agricultural systems has been regarded as a cost-effective and environmentally friendly strategy for ensuring food security and offsetting anthropogenic carbon dioxide emission (Lal, 2004). Among the numerous recommended management practices for sequestering C in cropping systems, residue retention has attracted great attention (Freibauer et al., 2004). It is estimated that every year 3.8 billion tons of crop residues are produced globally (Thangarajan et al., 2013), and a total potential of 0.6–1.2 Pg C can be sequestered by returning crop residues to soils (Lal, 2009).

Based on a meta-analysis of a global dataset from 176 studies, Liu et al. (2014) indicated that crop residue incorporation significantly increased SOC concentration by 12.8% on average, in soils with initial SOC concentration of 2–35 g kg<sup>-1</sup>. Likewise, Zhao et al. (2015)

conducted a meta-analysis and found that SOC concentration could be increased by 0.81 g kg<sup>-1</sup> at 0–30 cm depth with crop retention in China. However, as shown in the above two studies, there were large differences in the magnitude and even the direction of the responses of SOC contents to residue retention. For example, Poeplau et al. (2015) reported that the effects on improving SOC content were negligible with aboveground residue amendment of barley, wheat, and oat in six Swedish long-term experiments. Reicosky et al. (2002) also found no increase in SOC stocks after long-term returning of maize residues. Decreases in SOC content after residue application have also been observed in previous studies in China (e.g. Wang et al., 2011).

The responses of SOC dynamics to crop residue input can be regulated by many factors, such as moisture, temperature, and soil properties, of which the type of crop residues is an important determinant (Bradford et al., 2016). Many studies have proposed that different organic materials with various chemical compositions may show different behaviors during decomposition in the same soils (Jensen et al., 2005; Powers et al., 2009; Bonanomi et al., 2011). It is likely that crop residues with large amounts of easily degradable C can increase microbial activity, leading to enhanced SOC decomposition and thus counteracting the positive effects of crop residues on SOC content (Guenet et al., 2010). Therefore, it is critical to gain insight into the chemical compositions of different types of crop residues to clarify their distinct impacts on soil C cycling.

Cellulose, hemicellulose, and lignin are three major biopolymers in crop residues (Valášková et al., 2007). These chemical compositions are traditionally analyzed by

extraction methods, which are useful but time-consuming (Kelleher et al., 2006). Over the past decades, non-destructive solid-state  $^{13}\text{C}$  crosspolarization magic angle spinning (CPMAS) nuclear magnetic resonance (NMR) spectroscopy has been frequently used to characterize the molecular compositions of organic matter (Baumann et al., 2009; Bonanomi et al., 2013). O-alkyl C and di-O-alkyl C (60–110 ppm), assigned to the monomeric units of cellulose and hemicellulose (De Marco et al., 2012), are preferentially consumed by r-strategists as C and energy resources (Clemente et al., 2013). Moreover, the resonances at 84 and 89 ppm were indicated to relate with the C-4 in the amorphous and crystalline cellulose, respectively (Martinez et al., 1999; Wikberg and Maunu, 2004). Davis et al. (1994a, b) reported that white rot fungi showed preference for the breakdown of amorphous cellulose, attributing to the easier penetration into amorphous over crystalline structure. In the cell walls of higher plants, lignin is chemically linked to cellulose and hemicellulose, encrusting carbohydrates from microbial degradation and providing resistance to environmental stress (Thevenot et al., 2010). In this case, lignin removal or modification is a prerequisite for the decomposition of lignin-shielded polysaccharides (Klotzbücher et al., 2013). As a complex macromolecular, lignin consists of vanillyl, syringyl, and cinnamyl monomers, each showing different methoxylation of the aromatic ring and each having distinct availability to microbes (White et al., 2016). Hence, investigating C substrate interactions and controlling components should illuminate the decomposition process of different crop residues.

Apart from the benefits of enhancing soil C level, applied residues can also be an important source of nutrient supply to crop growth. Nitrogen (N) in crop residues was

estimated at 46.3 Tg, equivalent to 56.3% of fertilizer N consumption across the world in 2001 (Lal, 2009). Thus, recycling N resources in crop residues to agricultural soils could partially substitute for energy-intensive and resource-reliant inorganic fertilizers (Abera et al., 2012). Factors driving organic material decomposition are also suggested to have impacts on N release (Varela et al., 2014). The C/N ratio of residues is commonly acknowledged as a main factor affecting microbial mineralization of N in crop residues (Vigil and Kissel, 1991; Tian et al., 1992). Trinsoutrot et al. (2000a) indicated that net N mineralization could occur when the C/N ratio of the decomposing residues was less than 24. Nonetheless, Parton et al. (2007) observed net N release when litter mass loss arrived at 60% and the average C/N ratio was lower than 40 in a 10-year field decomposition experiment. These inconsistent findings about C/N threshold for net N mineralization could be attributed to the differences in experimental conditions and duration, and also to the residue C and N characteristics (Abiven et al., 2005; Jensen et al., 2005; Gillis and Price, 2016). Trinsoutrot et al. (2000b) reported that the quantity of N released from roots, stems, and pod walls of *Brassica napus* L. were closely related to the initial N content. However, other researchers suggested that N mineralization was primarily dependent on the quality of organic C compounds (Piñeiro et al., 2006; Corre et al., 2007). There were close interactions between C and N compounds, for example, recalcitrant lignin can shield N from mineralization due to chemical binding or physical isolation (Boerjan et al., 2003; Talbot et al., 2012), and polyphenol-bound protein thus may result in N immobilization (Gentile et al., 2008). Consistently, Eldridge et al. (2017) found that the mineralized N from organic wastes was negatively related to the content of

aromatic and phenolic C. Therefore, C chemical compositions of the crop residues should be incorporated into N-management strategies on farmlands under residue retention.

The cultivated Mollisol in northeast China, with an area of 14.7 million hectare (Liu et al., 2012), is generally considered as inherently fertile, and plays a significant role in national grain production. However, an overall loss of 22.3% in SOC concentration has occurred in this region over the past three decades, mainly attributed to high erosion and low input of organic materials (Yan et al., 2011). In this case, returning crop residues to soil is recommended to mitigate SOC loss and recover soil fertility (Liu et al., 2014). In the study region, maize, soybean, and wheat are three staple crops (Qiao et al., 2014). Different types of residues may have different decomposition patterns and rates due to their various chemical compositions, which need to be understood to provide scientific supports for crop residue management in this region. In the present study, we evaluated the decomposition of these crop residues in a year-long litterbag experiment, and determined the chemical composition of organic C in the crop residues with the solid-state  $^{13}\text{C}$ -NMR technique. The main objectives of this study were to: (1) quantify the decay rate of maize, soybean, and wheat residues, (2) identify the critical C functional groups responsible for the decomposition differences both among residue types and at different decay stages, and (3) analyze N dynamics and its interactions with C decomposition during residue decay process.

## 2. Materials and methods

### 2.1. Study site

The study was carried out in a rainfed cropland in Hailun National Agro-ecological Experimental Station, Heilongjiang Province, China (47°26'N, 126°38'E). The region has a temperate continental monsoon climate. The mean annual air temperature is 1.9 °C and the mean annual precipitation is 560 mm from 1953 to 2013, based on the data of the National Meteorological Information Center (<http://cdc.nmic.cn/home.do>). Air and soil (10 cm depth) temperature and precipitation during the study period (from 21 May 2013 to 21 May 2014) were obtained from a meteorological station nearby. The soil is a Typic Hapludolls (US soil taxonomy) derived from loamy loess with 8% sand, 72% silt, and 20% clay at the surface depth (0–20 cm). The soil pH was 6.0. The soil had 28.3 g kg<sup>-1</sup> total organic C, 2.1 g kg<sup>-1</sup> total N, 3.2 mg N kg<sup>-1</sup> ammonium (NH<sub>4</sub><sup>+</sup>), and 8.7 mg N kg<sup>-1</sup> nitrate (NO<sub>3</sub><sup>-</sup>) prior to the establishment of our experiment.

## 2.2. Experimental design

In the study area, field is cultivated with a single crop per year and the main crops are maize (*Zea mays* L.), soybean (*Glycine max* L.), and wheat (*Triticum aestivum* L.), which are planted in spring and harvested in autumn. After harvest, the aboveground biomass (including stems and leaves) of three crops were dried at 60 °C for 48 h, cut into 2-cm length, and individually mixed for homogenization. Crop residue decay was studied with the standardized litterbag method (Aerts, 1997). Every type of residue (40 g on oven-dried basis) was separately filled into each litterbag. The litterbags were 0.15 m × 0.20 m with 0.25-mm mesh nylon netting, and the bag edges were sealed with a fishing line and linked to a marker. On 21

May 2013, a total of 48 litterbags (3 residue types  $\times$  4 replicates  $\times$  4 sampling times) were randomly and horizontally buried at the 10-cm depth in soil, and the marker was left on the soil surface to assist sampling. The distance between the litterbags was  $\sim$ 20 cm. The bags were retrieved on 21 June 2013 (1 month), 21 August 2013 (3 months), 21 October 2013 (5 months), and 21 May 2014 (12 months). At every recovery, the adhering soil particles were carefully brushed off from the litterbags, and the inside residues were taken out and gently shaken over a 1-mm sieve to eliminate the interfusion of soil. The cleaned residues were dried at 60 °C for 48 h and weighed for the remaining mass. Subsamples of the dried residues were ground through a 0.15- $\mu$ m sieve for C and N content and  $^{13}\text{C}$ -NMR analysis.

### *2.3. Analyses of soil and crop residue samples*

Soil particle size was measured on a laser particle size analyzer (LS13320, Beckman Coulter, Brea, USA). Soil moisture content was determined with a time domain reflectometry probe during the non-frozen period in the study plot, and was expressed as water-filled pore space (WFPS) calculated with soil bulk density ( $1.0 \text{ g cm}^{-3}$ ). Soil pH value was measured in a 1:2.5 soil to water ratio. The C and N concentrations of soil and residues were determined by combustion oxidation on a CN analyzer (Vario Max CN, Elementar, Hanau, Germany). The soil  $\text{NH}_4^+$  and  $\text{NO}_3^-$  concentration were analyzed using continuous-flow autoanalyzer (San++, Breda, the Netherlands) after extraction with 2 M potassium chloride.

Chemical composition of the residues was determined with solid-state  $^{13}\text{C}$ -NMR spectroscopy under the same condition, allowing a quantitative comparison among residue

types (Bonanomi et al., 2011). The cross polarization magic angle spinning technique was employed on a Bruker Avance III 400 spectrometer (Bruker BioSpin Corporation, Switzerland) operating at a  $^{13}\text{C}$  resonance frequency of 100.6 MHz. Subsamples were weighed into a 4-mm zircon oxide rotor with Kel-F end caps and spun at 14 kHz. NMR spectra were obtained with 2 s of recycle delay, 1.5 ms of contact time, 10 ms of acquisition time, and 1000 scans. Carbon chemical shifts were referenced to the methylene signal (29.5 ppm) of solid adamantane as an external standard.

The  $^{13}\text{C}$ -NMR spectra were processed with MestReNova version 8 (Mestrelabs Research, Santiago de Compostela, Spain). Each  $^{13}\text{C}$ -NMR spectrum was segmented into seven chemical shift regions: 0–45, 45–60, 60–93, 93–110, 110–142, 142–160, and 160–190 ppm, assigned to seven C functional groups, namely, alkyl C, methoxyl C, O-alkyl C, di-O-alkyl C, aromatic C, phenolic C, and carbonyl C, respectively (Table 1). Although the signals for methoxyl C and N-alkyl C were overlapped in the 45–60 ppm region, we labelled them as the methoxyl C on account of the progressive increase during the decay process (Xu et al., 2017a). The O-alkyl C/alkyl C ratio and aromaticity  $((110\text{--}160 \text{ ppm}) / (0\text{--}160 \text{ ppm}) \times 100)$  were calculated and regarded as robust indicators of residue decomposition degree (Dias et al., 2013). Lignin concentration was estimated using the model of Haw et al. (1984). The syringyl to guaiacyl (S/G) ratio was calculated as the signal ratio of 153 ppm to 147 ppm, and the crystallinity of cellulose was evaluated by the signal ratio of 89 ppm to 84 ppm (Albrecht et al., 2008).

#### 2.4. Data and statistical analysis

The remaining C of crop residues in the litterbag after a certain decomposition time was calculated as the remaining mass of residue multiplied by its C concentration. The remaining mass of **seven C functional groups** was estimated as the remaining C multiplied by the relative abundance of C **functional groups** from the  $^{13}\text{C}$ -NMR data (Ono et al., 2013). The mass losses of residues, total C, and **seven C functional groups** over time could be described by an exponential decay model (Rodríguez Pleguezuelo et al., 2009):

$$M_t = M_0 \times e^{-kt} \quad (1)$$

where  $M_0$  is the initial mass of residues, total C, and **seven C functional groups** at time 0;  $M_t$  is the remaining mass of residues, total C, and **seven C functional groups** at time  $t$ ; and  $t$  (month) is the decomposition time from residue burial to sampling time. According to equation (1), the decomposition rate ( $k$ ,  $\text{month}^{-1}$ ) was calculated as follows:

$$k = -1/t \times \ln (M_t / M_0) \quad (2)$$

The proportion ( $P$ , %) of decomposed C was calculated as:

$$P = (1 - RM \times RC / IM \times IC) \times 100 \quad (3)$$

where  $RM$  and  $IM$  is the remaining and initial residue mass, respectively;  $RC$  and  $IC$  is the C concentration in remaining and initial residues, respectively. Similarly, the proportion of released N was calculated.

The remaining mass and decomposition rate of residues, the remaining C and N, C/N ratio, and C chemical compositions of residues were analyzed by two-way analysis of variance (ANOVA) to determine the effects of residue type and decomposition time and their

interaction. Non-metric multidimensional scaling (NMDS) analysis was performed to describe the effects of residue types and decomposition time on C composition changes during the residue decay process. Pearson analysis was conducted to examine for the correlation between the C chemical compositions with the variation along NMDS axis 1 and 2, and with the decomposition rate of residues. Linear regression models were fitted to describe the relationships between the proportion of decomposed C or released N and the mass loss of **seven C functional groups**. The normality and homogeneity of variance of data were tested using the Kolmogorov-Smirnov test and Levene statistic, respectively. All statistical analyses were conducted with SPSS (SPSS Inc., Chicago, IL, USA) and Origin Pro 8.5 (OriginLab, USA) with significant differences accepted at  $P \leq 0.05$ , with the exception that the NMDS analysis was performed with the vegan package of R version 3.1.0 (R Foundation for Statistical Computing, Vienna, Austria).

### **3. Results**

#### *3.1. Environmental conditions*

The mean daily air temperature during the experiment was 3 °C. The highest air temperature was 26 °C observed on 24 June 2013 and the lowest was -30 °C on 12 January 2014 (Fig. 1). Soil temperature varied from -4 °C to 24 °C, and coincided with changes in air temperature except the frozen period when soil temperature was substantially higher than air temperature due to insulation of the snow cover. The annual precipitation was 888 mm, 81% of which fell from June to August in summer 2013. Snow began to accumulate on 9

November 2013, and completely melted on 16 March 2014. The soil moisture content ranged between 33% and 92% WFPS during the experimental period. Increased WFPS was generally observed after rainfall, particularly after the rainstorm event (daily rainfall was 178 mm) on 30 July 2013, which made soil nearly saturated for about one month.

### 3.2. Remaining mass, C, and N, and the C/N ratio

The remaining mass of maize and soybean residues sharply decreased to 52% and 45%, respectively, of the initial mass during the first 3 months of decomposition, and leveled off for the rest of the experimental period (Fig. 2a). The fast decomposition phase of wheat residues extended over 5 months, reducing to 47% of its initial mass. Generally, soybean had significantly ( $P < 0.05$ ) lower remaining mass than maize and wheat during the experimental period. After a year-long decomposition, the proportion of the remaining mass was 43%, 48%, and 55%, respectively, for soybean, maize, and wheat residues. Residue type and decomposition time had a significant ( $P < 0.001$ ) interaction on remaining mass (Fig. 2a). The decomposition rates of residues significantly ( $P < 0.001$ ) varied among decomposition time, decreasing from 0.223–0.379 month<sup>-1</sup> during the first month to 0.054–0.076 month<sup>-1</sup> within 12 months, except that of wheat keeping relatively steady within 3 months compared with 5 months (Table 2). Residue type also significantly ( $P < 0.001$ ) affected the decomposition rate. Generally, soybean had significantly ( $P < 0.05$ ) larger decomposition rate than maize and wheat (except within 5 months) during the decay process.

The remaining C in residues showed a similar changing pattern as the remaining mass

(Fig. 2b). There were significant effects ( $P < 0.001$ ) of residue type, decomposition time, and their interaction on remaining C. At the end of experiment, the soybean residues retained 37% of the initial C, followed by maize (40%) and wheat (43%) residues. The remaining N in soybean and maize residues decreased quickly during the first 3 months of decomposition, followed by a slight increase after 5 months and then a decrease after 12 months (Fig. 2c). However, wheat residues exhibited a decrease in remaining N during the first 5 months, and then a slight increase. After 12 months, the remaining N was 69%, 73%, and 78%, respectively, in maize, soybean, and wheat residues, indicating a net N release for all crop residues. The C/N ratio significantly ( $P < 0.001$ ) decreased from 41–57 to 23–32 across all residue types over the first 5 months, but did not change significantly thereafter until the end of experiment (Fig. 2d).

### 3.3. Changes in chemical composition of the decomposing residues

The relative abundance of seven C functional groups varied significantly ( $P < 0.001$ ; Fig. 3) among residue types and decomposition time. In the original residues, O-alkyl C, with relative abundance of 57–59%, dominated the  $^{13}\text{C}$ -NMR spectra, followed by di-O-alkyl C (Fig. 3a and b). During the decomposition period, the relative abundance of these two types of C significantly ( $P < 0.01$ ) decreased to 48–52% and to 11–12%, respectively, but other C types gradually increased. The O-alkyl C/alkyl C ratio gradually decreased from 8.8–11.6 to 6.0–8.5 (Table 3). The crystallinity of cellulose had a significant ( $P < 0.05$ ) initial increase followed by a decrease. Meanwhile, the aromaticity and lignin concentration increased, from

9.3–9.9% to 14.0–17.7% and from 11.1–11.8% to 17.0–22.0%, respectively. The S/G ratio slightly decreased from 1.5–1.9 to 1.3–1.5. Overall, the chemical differences among different residue types increased with the decomposition time (Fig. 3c). The variation along NMDS1 was significantly ( $P < 0.001$ ) negatively correlated with O-alkyl C and di-O-alkyl C, and positively related to alkyl C, methoxyl C, aromatic C, and phenolic C (Fig. 3d). The  $k$  value differed among seven C functional groups, decreasing in the following order: O-alkyl C > di-O-alkyl C > carbonyl C > alkyl C > methoxyl C > aromatic C > phenolic C. The decomposition rates of O-alkyl C, di-O-alkyl C, and carbonyl C were significantly ( $P < 0.001$ ) larger in soybean than in maize and wheat.

### *3.4. Relationships between residue decomposition and chemical composition*

The decomposition rate of residues correlated positively with C, C/N ratio, O-alkyl C, O-alkyl C/alkyl C ratio, cellulose crystallinity, and S/G ratio, and negatively with N, alkyl C, aromatic C, phenolic C, carbonyl C, aromaticity, and lignin ( $P < 0.05$ ; Table 4). The proportion of decomposed C was significantly related to the mass loss of O-alkyl C ( $P = 0.02$ ), di-O-alkyl C ( $P = 0.02$ ), and carbonyl C ( $P = 0.004$ ) (Fig. 5a–c). Significant relationships were also observed between the proportion of released N and the mass loss of alkyl C ( $P = 0.02$ ), O-alkyl C ( $P = 0.05$ ), and aromatic C ( $P = 0.04$ ) (Fig. 5d–f).

## **4. Discussion**

### *4.1. Crop residue decomposition as affected by climate conditions*

The annual mass loss of crop residues observed in our study were lower than those (71.2–77.0%, 77.1–85.5%, and 63.0–72.1% for maize, soybean, and wheat residues, respectively) measured in previous litterbag studies (Ghidey et al., 1985; Powell et al., 2009; Wang et al., 2012; Grandy et al., 2013; Wotherspoon et al., 2014). Climate conditions, mainly temperature and precipitation, are regarded as primary factors regulating the decomposition of organic materials among various sites (Bradford et al., 2016). At our study site, the mean air temperature was 3 °C during the experimental period (Fig. 1), which was substantially lower than 6–15.3 °C in those studies mentioned above. In warmer environments, the critical value of activation energy for microbial decomposition is more likely to be exceeded (Dungait et al., 2012). Therefore, the lower temperature, as compared to previous studies, might be an explanation for the lower mass loss of residues in our study. The annual precipitation was 888 mm in our study, which fell in the middle of the range (615–1185 mm) in the above comparative studies. However, during the present experiment, a summer rainstorm resulted in the soil moisture content > 90% WFPS, and this waterlogging condition continued almost throughout August in 2013 (Fig. 1). Anaerobic conditions might rapidly develop in the waterlogged soil, since the rate of oxygen diffusion through water is 10,000-fold lower than that in gas (Hamonts et al., 2013). In a previous study, we found that high moisture at WFPS > 60% could decrease microbial biomass and heterotrophic activity in the studied soil (Chen et al., 2017). As a consequence, the excessively wet condition induced by heavy rainstorm in this study might be another contributor for the observed lower mass loss of residues.

#### 4.2. Impacts of residue type and chemical composition on decomposition

We found that soybean residues had 9.9–26.0% more mass loss compared with maize and wheat residues over the experimental period (Fig. 2a). This finding was consistent with previous studies that showed mass loss was greater in soybean residues, followed by maize and wheat residues (Ghidey et al., 1985; Havis and Alberts, 1993; Grandy et al., 2013). The initial residue C/N ratio was 57 for soybean, which was similar to maize and higher than wheat (Fig. 2d). Generally, crop residues with higher C/N ratios were supposed to decompose more slowly than those with lower C/N ratios (Melillo et al., 1989; Heal et al., 1997; Johnson et al., 2007). However, the C/N ratio of litters was a useful indicator of substrate decomposability in N-poor rather than N-rich soils (Bonanomi et al., 2016). This indicator sometimes fails to describe the decomposition of organic substances, due to the simplistic use of total organic C and N without consideration of the chemical compositions of organic pools (Powers et al., 2009; Bonanomi et al., 2013). Indeed, we found that different C functional groups in residues had different decomposition rates, all showing clear distinction from that of the total organic C (Fig. 4).

The proportion of decomposed C in residues was significantly related with the mass loss of O-alkyl C, di-O-alkyl C, and carbonyl C (Fig. 5). The O-alkyl C and di-O-alkyl C, mainly associated with cellulose and hemicellulose (De Marco et al., 2012), was more decomposed in soybean than in maize and wheat residues (Fig. 4). These polysaccharides generally cross-link with lignin in plant cell walls, and thus the structure of lignin could determine the chemical protection and microbial availability of these labile C substrates (White et al., 2016). The

methoxyl substituent of syringyl (S) units in lignin is linked to the C5 of the aromatic ring, preventing the polymerization with another aromatic unit (Albrecht et al., 2008). Therefore, the syringyl units in lignin are formed with labile  $\beta$ -O-4 linkages which could be degraded quickly, but the lignin guaiacyl (G) units can polymerize to generate recalcitrant condensed aryl-aryl linkages (Bahri et al., 2006; Talbot et al., 2012). In this study, the soybean residues had relatively higher S/G ratio than the maize and wheat residues (Table 3). Therefore, the larger decomposition rates of O-alkyl C and di-O-alkyl C in the soybean residues might be due to the weaker protection of lignin. On the other hand, carbonyl C is acknowledged as critical biochemical constitution of the amide structures in proteins (Wang et al., 2004). Baumann et al. (2011) suggested that decomposition of wheat residues had a positive relationship with carbonyl C, a C functional group beneficial for microbial protein synthesis and proliferation. We found that the decomposition rate of carbonyl C was largest for the soybean residues in comparison with maize and wheat residues (Fig. 4). It is likely that higher availability of proteins in soybean residues facilitated microbial decomposition (Osaki et al., 1991).

As decomposition progressed, a wider disparity was observed in the organic C chemistry among the three types of crop residues (Fig. 3c). In contrast, Wallenstein et al. (2013) reported that litter chemistry converged during decomposition, due to the accumulation of microbial product that was similar among microbial species and dominant in the remaining mass. However, if the litters have contrasted initial content in chemically recalcitrant compounds, a chemical divergence would occur during decomposition, due to the difference

of accumulated litter-originated recalcitrant compounds while the labile C is consumed by microorganisms (Wickings et al., 2012). Consistently, we found that residue chemical divergence had significant correlations with the relative decrease in labile O-alkyl C and di-O-alkyl C, and the relative increase in recalcitrant aromatic C, phenolic C, and methoxyl C (Fig. 3d). For example, the aromatic C was similar in initial crop residues, ranging at 5.8–6.2%, and increased to 8.5–10.4% at the end of experiment, exhibiting a larger variation. Therefore, the increase of chemical divergence among crop residues in our study might result from the differences in the concentration and composition of recalcitrant C compounds (Parsons et al., 2014). In addition, the appearance of chemical convergence or divergence was suggested to be dependent on the undergoing decay stage (Wallenstein et al., 2013). In our study, the C chemical divergence was observed during one year, and long-term studies are needed to confirm these findings.

### *4.3. Temporal pattern of residue decomposition and related determinants*

The decomposition rate of residues significantly decreased from 0.223–0.379 month<sup>-1</sup> during the first month to 0.054–0.076 month<sup>-1</sup> over a year of decomposition (Table 2). We found that the decomposition rate of residues had a close correlation with the change of O-alkyl C (Table 4). In crop residues, O-alkyl C is usually a major constituent of the most abundant compound cellulose, and preferentially consumed by microorganisms to gain energy (Xu et al., 2017b). Interestingly, the cellulose crystallinity, expressed by the ratio of crystalline to amorphous cellulose (Albrecht et al., 2008), exhibited a significant increase

during the first 3 months of decomposition (Table 3). Park et al. (2010) pointed out that decomposition of cellulose was affected by its crystallinity, and amorphous cellulose was supposed to be digested more easily by enzymes than crystalline cellulose. Hence, high content of cellulose especially those with amorphous structure were responsible for initial large decomposition rate of residues. Meanwhile, in the presence of abundant available C substrates, the aromatic polymer lignin could be co-metabolized by white-rot fungi (Rutigliano et al., 1996; Klotzbücher et al., 2013). There was a positive correlation between the decomposition rate of residues and S/G ratio of lignin (Table 4). The syringyl (S) units in lignin were suggested to be preferentially degraded over guaiacyl (G) units as discussed above. Thus, high S/G ratio of lignin could also partly contribute to high decomposition rate of residues during initial stages.

As residue decomposition progressed, the lignin concentration and aromaticity of residues gradually increased (Table 3), which in turn negatively affected the decomposition of residues (Table 4). In accordance with our findings, Berg and Matzner (1997) indicated a critical role of lignin in controlling decomposition rates after 30–40% of the litter mass was lost. As a three-dimensional macromolecule, lignin had inherently low reactivity and required high activation energy to be decomposed (Kögel-Knabner, 2002; Davidson and Janssens, 2006). However, during the late decomposition period from 21 October 2012 to 21 May 2013, soil temperature dropped below 0 °C (Fig. 1). Microorganisms in frozen soils had to synthesize molecular chaperones, such as proteins and trehalose, to survive at low temperature (Schimel and Mikan, 2005). Considering the limited labile C resources in the residues at this time (Fig.

3a and b) and cold temperature stress on microbial physiology, there were little possibilities to meet the energy demands of lignin degradation during the late decomposition stage.

In the present study, the initial C/N ratios of residues were 41–57, and N release from residue pool occurred over the entire decomposition duration, particularly at the initial stage (Fig. 2). It is traditionally acknowledged that microbial N immobilization is predominant over N mineralization when C/N ratio of the organic materials is above the theoretical value of approximately 25 (Trinsoutrot et al., 2000a). However, in line with our findings, Moore et al. (2006) also indicated that net N release started even when the average C/N ratio of litters was about 55 (a range of 37–71) in the decomposing litters of Canadian upland forests. Piñeiro et al. (2006) proposed that an overall C/N ratio could not indicate net N mineralization or immobilization, because different fractions in organic matter had different C/N ratios.

The chemical composition may play an important role in regulating N transformations during organic matter decomposition (Corre et al., 2007; Eldridge et al., 2017). Over a year of decomposition, the released N increased linearly with the increasing mass loss of O-alkyl C, alkyl C, and aromatic C (Fig. 5). Alkyl C is usually found in lipids, cutin, and suberin (Bonanomi et al., 2013), and aromatic C is a main unit of tannin and lignin (Lorenz et al., 2000). It is likely that microorganisms mined N from recalcitrant compounds at the expense of labile C, as they may have limited access to N nutrient in the soil environment outside the litterbags (Craine et al., 2007). On the other hand, alkyl C and aromatic C also constitute relatively high-quality (high susceptibility to microbial degradation) substrates, such as aromatic amino acids (Erhagen et al., 2013). In such case, alkyl C and aromatic C could

represent the organic N origin, and thus were responsible for net N release in decomposing residues (Rowell et al., 2001).

#### *4.4. Implications for SOC sequestration and N fertilizer management*

The cultivated Mollisol of northeast China has suffered from SOC loss over the past several decades, partly due to the removal of crop residues after harvest (Yan et al., 2011). Qiao et al. (2014) reported that the annual residue biomass was 6.45, 2.36, and 2.66 Mg ha<sup>-1</sup> for maize, soybean, and wheat, respectively, at the same study site of this study. Based on the data of C decomposition rate in our one-year litterbag experiment, full residue retention for maize, soybean, and wheat was estimated to contribute 1.10, 0.37, and 0.48 Mg C ha<sup>-1</sup>, respectively, to SOC stock during the first year after application (Fig. 6). In a 8-year field trial in northeast China, You et al. (2017) found that the annual SOC sequestration induced by maize and soybean residue retention was 0.80 Mg C ha<sup>-1</sup>. As Chen et al. (2017) measured in-situ, the studied soil lost 1.88 Mg C ha<sup>-1</sup> year<sup>-1</sup> through microbial respiration from a field under conventional management without crop residue retention. Therefore, residue retention is likely to make a significant contribution to the mitigation of SOC loss, offsetting 19.5–58.5% of SOC loss in the first year after application. However, to balance or increase SOC stock, more input of organic materials such as organic manures is required (Xu et al., 2017a). The annual N release from the crop residue decomposition was estimated at 5–16 kg N ha<sup>-1</sup> during the first year following residue retention (Fig. 6). This suggested that applied residues might be a potentially available N source for plant growth in the studied cropland, although this

represents only a minor contributor to annual crop N uptake amount.

However, cautions should be taken when extrapolating our findings, considering the possible artifacts associated with the litterbag approach. For example, the microclimate conditions and microbial community structure may be different in litterbag and soil, and litterbag approach may favor N mineralization over immobilization since it limits the contact between crop residues and soil mineral N. High uncertainty may exist in our calculation of SOC sequestration contribution and N release amount from crop residue decomposition, as they may decline in the subsequent years and also differ from the direct measurement of soil C or N stock changes (Mosier et al., 2005). This calculation may also overestimate the C sequestration induced by residues since it does not take into account the acceleration of microbial mineralization of pre-existent soil C, i.e., priming effect (Fontaine et al, 2011). In addition, our results are obtained from a single soil-climate system. It is very likely that there are complex interactions between residue chemistry, climate, soil properties, management practices, and soil fauna and microbial communities, which may collectively exert significant impacts on the decomposition of residues. Therefore, experiments across different sites and years are needed to further examine the decomposition of crop residues in the field and evaluate their effects on soil C sequestration and N supply.

## 5. Conclusions

Our results emphasized the need to consider organic carbon chemistry of different types of residues when investigating their decomposition process. In the first year after residue

retention, mass loss was highest for the soybean residues, followed by maize and wheat residues. The proportion of decomposed C had close positive relationships with the mass loss of O-alkyl C, di-O-alkyl C, and carbonyl C, the decomposition rates of which were larger in soybean than maize and wheat residues. Moreover, the soybean residues had larger syringyl/guaiacyl ratio in lignin, indicating higher availability to microorganisms. The decomposition rate of residues decreased from 0.223–0.379 month<sup>-1</sup> within the first month to 0.054–0.076 month<sup>-1</sup> over the entire 12 months, with increasing aromaticity and lignin concentration in the residues. As decomposition progressed, divergence in the C chemistry was observed among the different types of residues. N release occurred throughout the decomposition period, which was related to the mass loss of alkyl C, O-alkyl C, and aromatic C. The fate of this released N is unknown since it might be transferred in mineral N pool, microbial biomass, in soil organic matter or be lost by leaching and denitrification. Soil C accumulation of 0.37–1.10 Mg C ha<sup>-1</sup> year<sup>-1</sup> could be achieved with full retention of the crop residues. Therefore, continuous residue retention could help to partly but not completely mitigate soil C loss and recover soil fertility in the cultivated Mollisol of northeast China. Further studies on retention of crop residues on farmlands, especially long term experiments at larger scales, are recommended to extend our findings. Research focusing on the interactions between C compounds, environmental conditions, and the functional microbial communities is required to improve understanding of the process and regulating factors of crop residue decomposition.

## Acknowledgements

Funding for this work was provided by the Chinese Academy of Sciences (XDB15020100) and the National Natural Science Foundation of China (31561143011). We would like to thank the staff at Hailun National Agro-ecological Experimental Station, Chinese Academy of Sciences for great logistic support and helpful assistance in the field experiment. Many thanks also to Chief Editor Prof. Petra Marschner and two anonymous reviewers for their valuable comments and suggestions that helped us to improve the manuscript quality greatly.

## References

- Abera, G., Wolde-meskel, E., Bakken, L.R., 2012. Carbon and nitrogen mineralization dynamics in different soils of the tropics amended with legume residues and contrasting soil moisture contents. *Biology and Fertility of Soils* 48, 51–66.
- Abiven, S., Recous, S., Reyes, V., Oliver, R., 2005. Mineralisation of C and N from root, stem and leaf residues in soil and role of their biochemical quality. *Biology and Fertility of Soils* 42, 119–128.
- Aerts, R., 1997. Climate, leaf litter chemistry and leaf litter decomposition in terrestrial ecosystems: a triangular relationship. *Oikos* 79, 439–449.
- Albrecht, R., Ziarelli, F., Alarcón-Gutiérrez, E., Le Petit, J., Terrom, G., Perissol, C., 2008. <sup>13</sup>C solid-state NMR assessment of decomposition pattern during co-composting of sewage sludge and green wastes. *European Journal of Soil Science* 59, 445–452.
- Bahri, H., Dignac, M.F., Rumpel, C., Rasse, D.P., Chenu, C., Mariotti, A., 2006. Lignin

turnover kinetics in an agricultural soil is monomer specific. *Soil Biology and Biochemistry* 38, 1977–1988.

Baumann, K., Marschner, P., Kuhn, T.K., Smernik, R.J., Baldock, J.A., 2011. Microbial community structure and residue chemistry during decomposition of shoots and roots of young and mature wheat (*Triticum aestivum* L.) in sand. *European Journal of Soil Science* ~~Eur. J. Soil Sci.~~ 62, 666–675.

Baumann, K., Marschner, P., Smernik, R.J., Baldock, J.A., 2009. Residue chemistry and microbial community structure during decomposition of eucalypt, wheat and vetch residues. *Soil Biology and Biochemistry* ~~Soil Biol. Biochem.~~ 41, 1966–1975.

Berg, B., Matzner, E., 1997. Effect of N deposition on decomposition of plant litter and soil organic matter in forest systems. *Environmental Reviews* 5, 1–25.

Boerjan, W., Ralph, J., Baucher, M., 2003. Lignin biosynthesis. *Annual Review of Plant Biology* 54, 519–546.

Bonanomi, G., Cesarano, G., Gaglione, S.A., Ippolito, F., Sarker, T., Rao, M.A., 2016. Soil fertility promotes decomposition rate of nutrient poor, but not nutrient rich litter through nitrogen transfer [Ding1]. *Plant Soil*, 412, 3974–41145.

Bonanomi, G., Incerti, G., Barile, E., Capodilupo, M., Antignani, V., Mingo, A., Lanzotti, V., Scala, F., Mazzoleni, S., 2011. Phytotoxicity, not nitrogen immobilization, explains plant litter inhibitory effects: evidence from solid-state <sup>13</sup>C NMR spectroscopy. *New Phytologist* 191, 1018–1030.

Bonanomi, G., Incerti, G., Giannino, F., Mingo, A., Lanzotti, V., Mazzoleni, S., 2013. Litter

quality assessed by solid state  $^{13}\text{C}$  NMR spectroscopy predicts decay rate better than C/N and lignin/N ratios. ~~Soil Biology and Biochemistry~~~~Soil Biol. Biochem.~~ 56, 40–48.

Bradford, M.A., Berg, B., Maynard, D.S., Wieder, W.R., Wood, S.A., 2016. Understanding the dominant controls on litter decomposition. ~~Journal of~~ Ecology 104, 229–238.

Chen, Z.M., Xu, Y.H., Zhou, X.H., Tang, J.W., Kuzyakov, Y., Yu, H.Y., Fan, J.L., Ding, W.X., 2017. Extreme rainfall and snowfall alter responses of soil respiration to nitrogen fertilization: a 3-year field experiment. ~~Glob~~al Change ~~Biolog~~y, <http://dx.doi.org/10.1111/gcb.13620>.

Clemente, J.S., Simpson, M.J., Simpson, A.J., Yanni, S.F., Whalen, J.K., 2013. Comparison of soil organic matter composition after incubation with maize leaves, roots, and stems. Geoderma 192, 86–96.

Corre, M.D., Brumme, R., Veldkamp, E., Beese, F.O., 2007. Changes in nitrogen cycling and retention processes in soils under spruce forests along a nitrogen enrichment gradient in Germany. ~~Glob~~al Change ~~Biolog~~y 13, 1509–1527.

Craine, J.M., Morrow, C., Fierer, N., 2007. Microbial nitrogen limitation increases decomposition. Ecology 88, 2105–2113.

Davidson, E.A., Janssens, I.A., 2006. Temperature sensitivity of soil carbon decomposition and feedbacks to climate change. Nature 440, 165–173.

Davis, M.F., Schroeder, H.A., Maciel, G.E., 1994a. Solid-state  $^{13}\text{C}$  nuclear magnetic resonance studies of wood decay III. Decay of Colorado blue spruce and paper birch by *Postia placenta*. Holzforschung 48, 301–307.

565 Davis, M.F., Schroeder, H.R., Maciel, G.E., 1994b. Solid-state  $^{13}\text{C}$  nuclear magnetic  
 566 resonance studies of wood decay I. White rot decay of Colorado blue spruce.  
 567 *Holzforschung* 48, 99–105.

568 De Marco, A., Spaccini, R., Vittozzi, P., Esposito, F., Berg, B., Virzo De Santo, A., 2012.  
 569 Decomposition of black locust and black pine leaf litter in two coeval forest stands on  
 570 Mount Vesuvius and dynamics of organic components assessed through proximate  
 571 analysis and NMR spectroscopy. Soil Biology and Biochemistry~~Soil Biol. Biochem.~~ 51,  
 572 1–15.

573 Dias, T., Oakley, S., Alarcón-Gutiérrez, E., Ziarelli, F., Trindade, H., Martins-Loução, M.A.,  
 574 Sheppard, L., Ostle, N., Cruz, C., 2013. N-driven changes in a plant community affect  
 575 leaf-litter traits and may delay organic matter decomposition in a Mediterranean maquis.  
 576 Soil Biology and Biochemistry~~Soil Biol. Biochem.~~ 58, 163–171.

577 Dungait, J.A.J., Hopkins, D.W., Gregory, A.S., Whitmore, A.P., 2012. Soil organic matter  
 578 turnover is governed by accessibility not recalcitrance. ~~Glob~~al- Change ~~Biolog~~y- 18,  
 579 1781–1796.

580 Eldridge, S.M., Chen, C.R., Xu, Z.H., Chan, K.Y., Boyd, S.E., Collins, D., Meszaros, I., 2017.  
 581 Plant available N supply and recalcitrant C from organic soil amendments applied to a  
 582 clay loam soil have correlations with amendment chemical composition. *Geoderma* 294,  
 583 50–62.

584 Erhagen, B., Öquist, M., Sparrman, T., Haei, M., Ilstedt, U., Hedenström, M., Schleucher, J.,  
 585 Nilsson, M.B., 2013. Temperature response of litter and soil organic matter decomposition

is determined by chemical composition of organic material. ~~Global~~ Change ~~Biology~~ 19,  
3858–3871.

Fontaine, S., Henault, C., Aamor, A., Bdioui, N., Bloor, J.M.G., Maire, V., Mary, B.,  
Revaillot, S., Maron, P.A., 2011. Fungi mediate long term sequestration of carbon and  
nitrogen in soil through their priming effect. ~~Soil Biology and Biochemistry~~~~Soil Biol.~~  
~~Biochem.~~ 43, 86–96.

Freibauer, A., Rounsevell, M.D.A., Smith, P., Verhagen, J., 2004. Carbon sequestration in the  
agricultural soils of Europe. *Geoderma* 122, 1–23.

Gentile, R., Vanlauwe, B., Chivenge, P., Six, J., 2008. Interactive effects from combining  
fertilizer and organic residue inputs on nitrogen transformations. ~~Soil Biology and~~  
~~Biochemistry~~~~Soil Biol. Biochem.~~ 40, 2375–2384.

Ghidey, F., Gregory, J.M., McCarty, T.R., Alberts, E.E., 1985. Residue decay evaluation and  
prediction. ~~Transactions of the American Society of Agricultural Engineers~~~~Trans. Am.~~  
~~Soc. Agric. Eng.~~ 28, 102–105.

Gillis, J.D., Price, G.W., 2016. Linking short-term soil carbon and nitrogen dynamics:  
environmental and stoichiometric controls on fresh organic matter decomposition in  
agroecosystems. *Geoderma* 274, 35–44.

Grandy, A.S., Salam, D.S., Wickings, K., McDaniel, M.D., Culman, S.W., Snapp, S.S., 2013.  
Soil respiration and litter decomposition responses to nitrogen fertilization rate in no-till  
corn systems. ~~Agriculture~~, ~~Ecosystems~~, ~~and~~ ~~Environment~~ 179, 35–40.

Guenet, B., Neill, C., Bardoux, G., Abbadie, L., 2010. Is there a linear relationship between

priming effect intensity and the amount of organic matter input? *Applied Soil Ecology* 46, 436–442.

Hamonts, K., Clough, T.J., Stewart, A., Clinton, P.W., Richardson, A.E., Wakelin, S.A., O’Callaghan, M., Condron, L.M., 2013. Effect of nitrogen and waterlogging on denitrifier gene abundance, community structure and activity in the rhizosphere of wheat. *FEMS Microbiology Ecology* 83, 568–584.

Havis, R.N., Alberts, E.E., 1993. Nutrient leaching from field-decomposed corn and soybean residue under simulated rainfall. *Soil Science Society of America Journal* 57, 211–218.

Haw, J.F., Maciel, G.E., Schroeder, H.A., 1984. Carbon-13 nuclear magnetic resonance spectrometric study of wood and wood pulping with cross polarization and magic-angle spinning. *Analytical Chemistry* 56, 1323–1329.

Heal, O.W., Anderson, J.M., Swift, M.J., 1997. Plant litter quality and decomposition: an historical overview. In Cadisch, G., Giller, K.E. (Eds.), *Driven by nature: plant litter quality and decomposition*, CAB International, Wallingford, pp. 47–66.

Jensen, L.S., Salo, T., Palmason, F., Breland, T.A., Henriksen, T.M., Stenberg, B., Pedersen, A., Lundström, C., Esala, M., 2005. Influence of biochemical quality on C and N mineralisation from a broad variety of plant materials in soil. *Plant Soil* 273, 307–326.

Jobbágy, E.G., Jackson, R.B., 2000. The vertical distribution of soil organic carbon and its relation to climate and vegetation. *Ecological Applications* 10, 423–436.

Johnson, J.M.F., Barbour, N.W., Weyers, S.L., 2007. Chemical composition of crop biomass impacts its decomposition. *Soil Science Society of America Journal* 71, 155–162.

- Kelleher, B.P., Simpson, M.J., Simpson, A.J., 2006. Assessing the fate and transformation of plant residues in the terrestrial environment using HR-MAS NMR spectroscopy. ~~Geochim. Cosmochim. Acta~~ Geochimica et Cosmochimica Acta 70, 4080–4094.
- Kögel-Knabner, I., 1997. <sup>13</sup>C and <sup>15</sup>N NMR spectroscopy as a tool in soil organic matter studies. *Geoderma* 80, 243–270.
- Kögel-Knabner, I., 2002. The macromolecular organic composition of plant and microbial residues as inputs to soil organic matter. ~~Soil Biology and Biochemistry~~ ~~Soil Biol. Biochem.~~ 34, 139–162.
- Klotzbücher, T., Kaiser, K., Filley, T.R., Kalbitz, K., 2013. Processes controlling the production of aromatic water-soluble organic matter during litter decomposition. Soil Biology and Biochemistry ~~Soil Biol. Biochem.~~ 67, 133–139.
- Lal, R., 2004. Soil carbon sequestration impacts on global climate change and food security. *Science* 304, 1623–1627.
- Lal, R., 2009. Soil quality impacts of residue removal for bioethanol production. *Soil and Tillage Research* 102, 233–241.
- Liu, C., Lu, M., Cui, J., Li, B., Fang, C.M., 2014. Effects of straw carbon input on carbon dynamics in agricultural soils: a meta-analysis. *Global Change Biology* 20, 1366–1381.
- Liu, X.B., Burras, C.L., Kravchenko, Y.S., Duran, A., Huffman, T., Morras, H., Studdert, G., Zhang, X.Y., Cruse, R.M., Yuan, X.H., 2012. Overview of Mollisols in the world: distribution, land use and management. ~~Canadian Journal of Soil Science~~ 92, 383–402.
- Lorenz, K., Preston, C.M., Raspe, S., Morrison, I.K., Feger, K.H., 2000. Litter decomposition

and humus characteristics in Canadian and German spruce ecosystems: information from  
tannin analysis and  $^{13}\text{C}$  CPMAS NMR. Soil Biology and Biochemistry ~~Soil Biol. Biochem.~~  
32, 779–792.

Martinez, A.T., Almendros, G., Gonzalez-Vila, F.J., Frund, R., 1999. Solid-state  
spectroscopic analysis of lignins from several Austral hardwoods. Solid State Nuclear  
Magnetic Resonance 15, 41–48.

Melillo, J.M., Aber, J.D., Linkins, A.E., Ricca, A., Fry, B., Nadelhoffer, K.J., 1989. Carbon  
and nitrogen dynamics along the decay continuum: plant litter to soil organic matter. Plant  
Soil 115, 189–198.

Moore, T.R., Trofymow, J.A., Prescott, C.E., Fyles, J., Titus, B.D., 2006. Patterns of carbon,  
nitrogen and phosphorus dynamics in decomposing foliar litter in Canadian forests.  
Ecosystems 9, 46–62.

Mosier, A.R., Halvorson, A.D., Peterson, G.A., Robertson, G.P., Sherrod, L., 2005.  
Measurement of net global warming potential in three agroecosystems. Nutrient  
Cycling in Agroecosystems 72, 67–76.

Ono, K., Hiradate, S., Morita, S., Hirai, K., 2013. Fate of organic carbon during  
decomposition of different litter types in Japan. Biogeochemistry 112, 7–21.

Osaki, M., Shinano, T., Tadano, T., 1991. Redistribution of carbon and nitrogen compounds  
from the shoot to the harvesting organs during maturation in field crops. Soil Science and  
Plant Nutrition 37, 117–128.

Park, S., Baker, J.O., Himmel, M.E., Parilla, P.A., Johnson, D.K., 2010. Cellulose

crystallinity index: measurement techniques and their impact on interpreting cellulase performance. *Biotechnology for Biofuels* 3, 10.

Parsons, S.A., Congdon, R.A., Lawler, I.R., 2014. Determinants of the pathways of litter chemical decomposition in a tropical region. *New Phytologist* 203, 873–882.

Parton, W., Silver, W.L., Burke, I.C., Grassens, L., Harmon, M.E., Currie, W.S., King, J.Y., Adair, E.C., Brandt, L.A., Hart, S.C., Fasth, B., 2007. Global-scale similarities in nitrogen release patterns during long-term decomposition. *Science* 315, 361–364.

Piñeiro, G., Oesterheld, M., Batista, W.B., Paruelo, J.M., 2006. Opposite changes of whole-soil vs. pools C:N ratios: a case of Simpson's paradox with implications on nitrogen cycling. *Global Change Biology* 12, 804–809.

Poeplau, C., Kätterer, T., Bolinder, M.A., Börjesson, G., Berti, A., Lugato, E., 2015. Low stabilization of aboveground crop residue carbon in sandy soils of Swedish long-term experiments. *Geoderma* 237–238, 246–255.

Powell, J.R., Levy-Booth, D.J., Gulden, R.H., Asbil, W.L., Campbell, R.G., Dunfield, K.E., Hamill, A.S., Hart, M.M., Lerat, S., Nurse, R.E., Pauls, K.P., Sikkema, P.H., Swanton, C.J., Trevors, J.T., Klironomos, J.N., 2009. Effects of genetically modified, herbicide-tolerant crops and their management on soil food web properties and crop litter decomposition. *Journal of Applied Ecology* 46, 388–396.

Powers, J.S., Montgomery, R.A., Adair, E.C., Brearley, F.Q., DeWalt, S.J., Castanho, C.T., Chave, J., Deinert, E., Ganzhorn, J.U., Gilbert, M.E., González-Iturbe, J.A., Bunyavejchewin, S., Grau, H.R., Harms, K.E., Hiremath, A., Iriarte-Vivar, S., Manzane,

E., De Oliveira, A.A., Poorter, L., Ramanamanjato, J.B., Salk, C., Varela, A., Weiblen, G.D., Lerda, M.T., 2009. Decomposition in tropical forests: a pan-tropical study of the effects of litter type, litter placement and mesofaunal exclusion across a precipitation gradient. ~~Journal of~~ Ecology 97, 801–811.

Qiao, Y.F., Miao, S.J., Han, X.Z., You, M.Y., Zhu, X., Horwath, W.R., 2014. The effect of fertilizer practices on N balance and global warming potential of maize–soybean–wheat rotations in Northeastern China. ~~Field Crops~~ Research 161, 98–106.

Reicosky, D.C., Evans, S.D., Cambardella, C.A., Allmaras, R.R., Wilts, A.R., Huggins, D.R., 2002. Continuous corn with moldboard tillage: residue and fertility effects on soil carbon. ~~Journal of~~ Soil and Water Conservation 57, 277–284.

Rodríguez Pleguezuelo, C.R., Durán Zuazo, V.H., Muriel Fernández, J.L., Martín Peinado, F.J., Franco Tarifa, D., 2009. Litter decomposition and nitrogen release in a sloping Mediterranean subtropical agroecosystem on the coast of Granada (SE, Spain): effects of floristic and topographic alteration on the slope. ~~Agriculture~~ Ecosystems and Environment 134, 79–88.

Rowell, D.M., Prescott, C.E., Preston, C.M., 2001. Decomposition and nitrogen mineralization from biosolids and other organic materials: relationship with initial chemistry. ~~Journal of~~ Environmental Quality 30, 1401–1410.

Rutigliano, F.A., De Santo, A.V., Berg, B., Alfani, A., Fioretto, A., 1996. Lignin decomposition in decaying leaves of *Fagus sylvatica* L. and needles of *Abies alba* Mill. ~~Soil Biology and Biochemistry~~ Soil Biol. Biochem. 28, 101–106.

- Schimel, J.P., Mikan, C., 2005. Changing microbial substrate use in Arctic tundra soils through a freeze-thaw cycle. ~~Soil Biology and Biochemistry~~~~Soil Biol. Biochem.~~ 37, 1411–1418.
- Talbot, J.M., Yelle, D.J., Nowick, J., Treseder, K.K., 2012. Litter decay rates are determined by lignin chemistry. *Biogeochemistry* 108, 279–295.
- Thangarajan, R., Bolan, N.S., Tian, G.L., Naidu, R., Kunhikrishnan, A., 2013. Role of organic amendment application on greenhouse gas emission from soil. ~~Science of the Total Environment~~ 465, 72–96.
- Thevenot, M., Dignac, M.F., Rumpel, C., 2010. Fate of lignins in soils: a review. ~~Soil Biology and Biochemistry~~~~Soil Biol. Biochem.~~ 42, 1200–1211.
- Tian, G., Kang, B.T., Brussaard, L., 1992. Biological effects of plant residues with contrasting chemical compositions under humid tropical conditions-decomposition and nutrient release. ~~Soil Biology and Biochemistry~~~~Soil Biol. Biochem.~~ 24, 1051–1060.
- Trinsoutrot, I., Recous, S., Bentz, B., Linères, M., Chèneby, D., Nicolardot, B., 2000a. Biochemical quality of crop residues and carbon and nitrogen mineralization kinetics under nonlimiting nitrogen conditions. ~~Soil Science Society of America Journal~~ 64, 918–926.
- Trinsoutrot, I., Recous, S., Mary, B., Nicolardot, B., 2000b. C and N fluxes of decomposing <sup>13</sup>C and <sup>15</sup>N *Brassica napus* L.: effects of residue composition and N content. ~~Soil Biology and Biochemistry~~~~Soil Biol. Biochem.~~ 32, 1717–1730.
- Valášková, V., Šnajdr, J., Bittner, B., Cajthaml, T., Merhautová, V., Hofrichter, M., Baldrian,

P., 2007. Production of lignocellulose-degrading enzymes and degradation of leaf litter by saprotrophic basidiomycetes isolated from a *Quercus petraea* forest. Soil Biology and Biochemistry ~~Soil Biol. Biochem.~~ 39, 2651–2660.

Varela, M.F., Scianca, C.M., Taboada, M.A., Rubio, G., 2014. Cover crop effects on soybean residue decomposition and P release in no-tillage systems of Argentina. Soil and Tillage Research 143, 59–66.

Vigil, M.F., Kissel, D.E., 1991. Equations for estimating the amount of nitrogen mineralized from crop residues. Soil Science Society of America Journal 55, 757–761.

Wallenstein, M.D., Haddix, M.L., Ayres, E., Steltzer, H., Magrini-Bair, K.A., Paul, E.A., 2013. Litter chemistry changes more rapidly when decomposed at home but converges during decomposition–transformation. Soil Biology and Biochemistry ~~Soil Biol. Biochem.~~ 57, 311–319.

Wang, J.B., Chen, Z.H., Chen, L.J., Zhu, A.N., Wu, Z.J., 2011. Surface soil phosphorus and phosphatase activities affected by tillage and crop residue input amounts. Plant, Soil and Environment 57, 251–257.

Wang, W.J., Baldock, J.A., Dalala, R.C., Moody, P.W., 2004. Decomposition dynamics of plant materials in relation to nitrogen availability and biochemistry determined by NMR and wet-chemical analysis. Soil Biology and Biochemistry ~~Soil Biol. Biochem.~~ 36, 2045–2058.

Wang, X.Y., Sun, B., Mao, J.D., Sui, Y.Y., Cao, X.Y., 2012. Structural convergence of maize and wheat straw during two-year decomposition under different climate conditions.

754 Environ~~mental~~- Sci~~ence and~~- Technol~~ogy~~- 46, 7159–7165.

755 White, K.E., Reeves Iii, J.B., Coale, F.J., 2016. Cell wall compositional changes during  
756 incubation of plant roots measured by mid-infrared diffuse reflectance spectroscopy and  
757 fiber analysis. *Geoderma* 264, 205–213.

758 Wickings, K., Grandy, A.S., Reed, S.C., Cleveland, C.C., 2012. The origin of litter chemical  
759 complexity during decomposition. *Ecol~~ogy~~- Letters*- 15, 1180–1188.

760 Wikberg, H., Maunu, S.L., 2004. Characterisation of thermally modified hard- and softwoods  
761 by C-13 CPMAS NMR. *Carbohydrate Polymers* ~~Carbohydr. Polym.~~-58, 461–466.

762 Wotherspoon, A., Thevathasan, N.V., Gordon, A.M., Voroney, R.P., 2014. Carbon  
763 sequestration potential of five tree species in a 25-year-old temperate tree-based  
764 intercropping system in southern Ontario, Canada. *Agrofor~~estry~~- Systems*- 88, 631–643.

765 Xu, Y.H., Chen, Z.M., Ding, W.X., Fan, J.L., 2017a. Responses of manure decomposition to  
766 nitrogen addition: role of chemical composition. *Sci-~~ence of the~~ Total Environ~~ment~~-*,  
767 <http://dx.doi.org/10.1016/j.scitotenv.2017.02.033>587–588, 11–21.

768 Xu, Y.H., Fan, J.L., Ding, W.X., Gunina, A., Chen, Z.M., Bol, R., Luo, J.F., Bolan, N., 2017b.  
769 Characterization of organic carbon in decomposing litter exposed to nitrogen and sulfur  
770 additions: links to microbial community composition and activity. *Geoderma* 286, 116–  
771 124.

772 Yan, X.Y., Cai, Z.C., Wang, S.W., Smith, P., 2011. Direct measurement of soil organic  
773 carbon content change in the croplands of China. *Glob-~~al~~ Change Biol~~ogy~~*- 17, 1487–  
774 1496.

775 You, M.Y., Li, N., Zou, W.X., Han, X.Z., Burger, M., 2017. Increase in soil organic carbon in  
776 a Mollisol following simulated initial development from parent material. European -  
777 Journal of- Soil Science- 68, 39–47.

778 Zhao, X., Zhang, R., Xue, J. F., Pu, C., Zhang, X.Q., Liu, S.L., Chen, F., Lal, R., Zhang, H.L.,  
779 2015. Management-induced changes to soil organic carbon in China: a meta-analysis.  
780 Advance in- Agronomy- 134, 1–50.

**Table 1** Signal assignment in the solid-state  $^{13}\text{C}$ -NMR spectra for crop residues (based on Kögel-Knabner, (1997), Wang et al. (2004), Baumann et al. (2009) and De Marco et al. (2012).

Chemical shift region (ppm)	C functional group	Major compounds represented
0–45	Alkyl C	Lipid, cutin, and suberin
45–60	Methoxyl C	Lignin substituent
60–93	O-alkyl C	Cellulose and hemicellulose
93–110	Di-O-alkyl C	Cellulose and hemicellulose
110–142	Aromatic C	Polyphenol, lignin, and tannin
142–160	Phenolic C	Polyphenol, lignin, and tannin
160–190	Carbonyl C	Carboxylic acid, amide, and organic acid

C, carbon;  $^{13}\text{C}$ -NMR,  $^{13}\text{C}$ -nuclear magnetic resonance.

**Table 2** Residue decomposition rate ( $k$ , month<sup>-1</sup>) after 1, 3, 5, and 12 months of decomposition, and results of ANOVA statistics testing the main effects and interactions of residue type and decomposition time.

Residue type	Decomposition time (months)			
	1	3	5	12
Maize	0.253 <sup>bA</sup> (0.018)	0.218 <sup>bB</sup> (0.001)	0.145 <sup>bC</sup> (0.007)	0.066 <sup>bD</sup> (0.001)
Soybean	0.379 <sup>aA</sup> (0.017)	0.269 <sup>aB</sup> (0.006)	0.164 <sup>aC</sup> (0.003)	0.076 <sup>aD</sup> (0.002)
Wheat	0.223 <sup>bA</sup> (0.012)	0.137 <sup>cB</sup> (0.009)	0.150 <sup>abB</sup> (0.003)	0.054 <sup>cC</sup> (0.001)
ANOVA analysis				
Source of variation	d.f.		<i>F</i> value	<i>P</i> value
Residue type	2		84.09	<0.001
Decomposition time	3		325.44	<0.001
Residue type × Decomposition time	6		20.12	<0.001

Decomposition rate values are means with standard errors ( $n = 4$ ). Lower case letters refer to vertical (residue type) comparisons. Upper case letters refer to horizontal (decomposition time) comparisons. Significant differences are accepted at  $P < 0.05$ .

791 **Table 3** Changes in the calculated indexes from  $^{13}\text{C}$ -NMR data of residues after 0, 1, 3, 5, and 12 months of decomposition.

Decomposition time (months)	Residue type	O-alkyl C/alkyl C	Crystallinity of cellulose	Aromaticity (%)	Lignin (%)	S/G
0	Maize	10.4 <sup>aAB</sup> (0.1)	0.53 <sup>bC</sup> (0.00)	9.4 <sup>aD</sup> (0.2)	11.2 <sup>aD</sup> (0.2)	1.50 <sup>aAB</sup> (0.16)
	Soybean	11.6 <sup>aA</sup> (2.3)	0.66 <sup>aB</sup> (0.01)	9.3 <sup>aD</sup> (1.1)	11.1 <sup>aC</sup> (1.4)	1.90 <sup>aA</sup> (0.10)
	Wheat	8.8 <sup>aA</sup> (0.0)	0.48 <sup>cB</sup> (0.01)	9.9 <sup>aD</sup> (0.1)	11.8 <sup>aD</sup> (0.2)	1.63 <sup>aA</sup> (0.12)
1	Maize	11.0 <sup>aA</sup> (0.4)	0.59 <sup>bA</sup> (0.01)	12.9 <sup>aB</sup> (0.3)	15.6 <sup>aB</sup> (0.3)	1.61 <sup>aA</sup> (0.10)
	Soybean	9.0 <sup>bB</sup> (0.4)	0.69 <sup>aAB</sup> (0.02)	12.7 <sup>aC</sup> (0.3)	15.4 <sup>aB</sup> (0.4)	1.79 <sup>aA</sup> (0.11)
	Wheat	7.6 <sup>cB</sup> (0.2)	0.49 <sup>cB</sup> (0.02)	12.1 <sup>aC</sup> (0.2)	14.6 <sup>aC</sup> (0.3)	1.61 <sup>aA</sup> (0.05)
3	Maize	10.0 <sup>aB</sup> (0.2)	0.56 <sup>bBC</sup> (0.01)	11.5 <sup>bC</sup> (0.1)	13.9 <sup>bC</sup> (0.1)	1.62 <sup>aA</sup> (0.09)
	Soybean	10.5 <sup>aAB</sup> (0.5)	0.71 <sup>aA</sup> (0.01)	15.4 <sup>aB</sup> (0.1)	18.9 <sup>aA</sup> (0.2)	1.66 <sup>aAB</sup> (0.04)
	Wheat	8.6 <sup>bA</sup> (0.2)	0.57 <sup>bA</sup> (0.02)	15.3 <sup>aA</sup> (0.4)	18.7 <sup>aA</sup> (0.5)	1.66 <sup>aA</sup> (0.08)
5	Maize	8.2 <sup>aC</sup> (0.2)	0.54 <sup>bC</sup> (0.01)	13.9 <sup>bA</sup> (0.4)	16.9 <sup>bA</sup> (0.5)	1.48 <sup>aAB</sup> (0.04)
	Soybean	7.0 <sup>bC</sup> (0.2)	0.66 <sup>aB</sup> (0.01)	17.9 <sup>aA</sup> (0.2)	22.3 <sup>aA</sup> (0.3)	1.63 <sup>aAB</sup> (0.06)
	Wheat	6.6 <sup>bC</sup> (0.3)	0.51 <sup>bB</sup> (0.01)	13.8 <sup>bB</sup> (0.5)	16.9 <sup>bB</sup> (0.7)	1.62 <sup>aA</sup> (0.06)
12	Maize	8.5 <sup>aC</sup> (0.2)	0.58 <sup>bAB</sup> (0.01)	14.0 <sup>cA</sup> (0.2)	17.0 <sup>cA</sup> (0.3)	1.26 <sup>bB</sup> (0.02)
	Soybean	7.0 <sup>bC</sup> (0.3)	0.69 <sup>aAB</sup> (0.03)	17.7 <sup>aA</sup> (0.4)	22.0 <sup>aA</sup> (0.5)	1.51 <sup>aB</sup> (0.08)
	Wheat	6.0 <sup>cC</sup> (0.2)	0.50 <sup>cB</sup> (0.01)	15.5 <sup>bA</sup> (0.2)	19.1 <sup>bA</sup> (0.2)	1.48 <sup>aA</sup> (0.06)

792 Values are means with standard errors (n = 4) in parentheses. Lower case letters refer to vertical comparisons between different residue types.

793 Upper case letters refer to vertical comparisons between different decomposition time. Significant differences are accepted at  $P < 0.05$ .

794 C, carbon;  $^{13}\text{C}$ -NMR,  $^{13}\text{C}$  nuclear magnetic resonance; S, syringyl units of lignin; G, guaiacyl units of lignin.

**Table 4** Pearson correlations between the residue decomposition rate and the chemical characteristics of residues over one-year decomposition.

Parameters	Correlation coefficient	<i>P</i> value
C	0.63	<0.001
N	−0.57	<0.001
C/N	0.71	<0.001
Alkyl C	−0.54	<0.001
Methoxyl C	−0.22	0.130
O-alkyl C	0.67	<0.001
Di-O-alkyl C	0.28	0.051
Aromatic C	−0.48	<0.001
Phenolic C	−0.36	0.011
Carbonyl C	−0.46	0.001
O-alkyl C/alkyl C	0.60	<0.001
Crystallinity of cellulose	0.36	0.012
Aromaticity	−0.46	<0.001
Lignin	−0.46	<0.001
S/G	0.54	<0.001

C, carbon; N, nitrogen; S, syringyl units of lignin; G, guaiacyl units of lignin.

## Figure legends

**Fig. 1.** Air temperature (AT), soil temperature (ST) at 10 cm depth, precipitation, soil water-filled pore space (WFPS), and depth of snow cover in the field from 21 May 2013 to 21 May 2014. Shade alongside the temperature line represents the highest and lowest values of daily air and soil temperature range.

**Fig. 2.** Dynamics of remaining (a) mass, (b) carbon (C), (c) nitrogen (N), and (d) the C/N ratio of residues in litterbags at different decomposition time. Vertical bars are standard errors ( $n = 4$ ). Results of ANOVA statistics testing the main effects and interaction of residue type and decomposition time are presented with  $F$ -values ( $*P < 0.05$ ,  $**P < 0.01$ ,  $***P < 0.001$ ).

**Fig. 3.** The carbon (C)-13 nuclear magnetic resonance signal intensity of **seven C functional groups**: (a) alkyl C and O-alkyl C, and (b) methoxyl C, di-O-alkyl C, aromatic C, phenolic C, and carbonyl C of residues at different decomposition time. Vertical bars are standard errors ( $n = 4$ ). Results of ANOVA statistics testing the main effects of residue type and decomposition time are presented with  $F$ -values ( $*P < 0.05$ ,  $**P < 0.01$ ,  $***P < 0.001$ ). (c) Non-multidimensional scaling (NMDS) analysis of the changes in residue chemistry throughout the decomposition period. Different colors represent different decomposition time. Different shapes indicate different residue types (square: maize; triangle: soybean; circle: wheat). (d) Correlations between **C functional groups** of residues and the loading scores alongside NMDS1 and NMDS2 axis. Significant correlations are shown in bold.

819

820 **Fig. 4.** Decomposition rate ( $k$ , month<sup>-1</sup>) of total organic C and seven C **functional groups** in  
821 residues over a year decomposition. Vertical bars are standard errors ( $n = 4$ ). Significant  
822 differences between residues at  $P < 0.05$  are indicated by different lowercase letters.

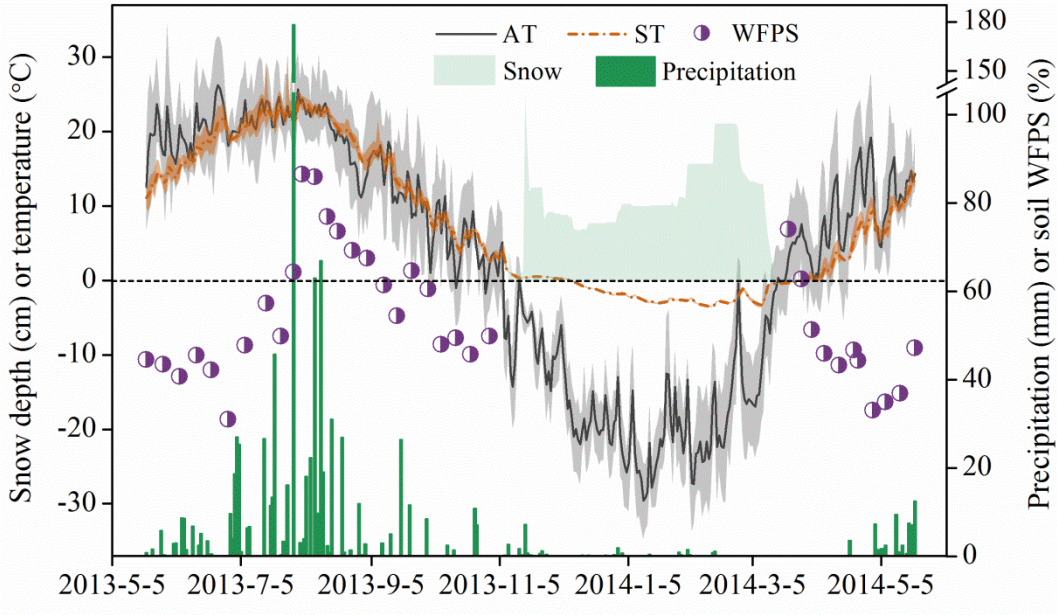
823

824 **Fig. 5.** Relationships between the proportion of decomposed carbon (C) and (a) mass loss of  
825 O-alkyl C, (b) mass loss of di-O-alkyl C, or (c) mass loss of carbonyl C, and between the  
826 proportion of released nitrogen (N) and (d) mass loss of alkyl C, (e) mass loss of O-alkyl C, or  
827 (f) mass loss of aromatic C during the experimental period. Dash-dot lines indicate the bounds  
828 of the 95% confidence intervals for the regression equations.

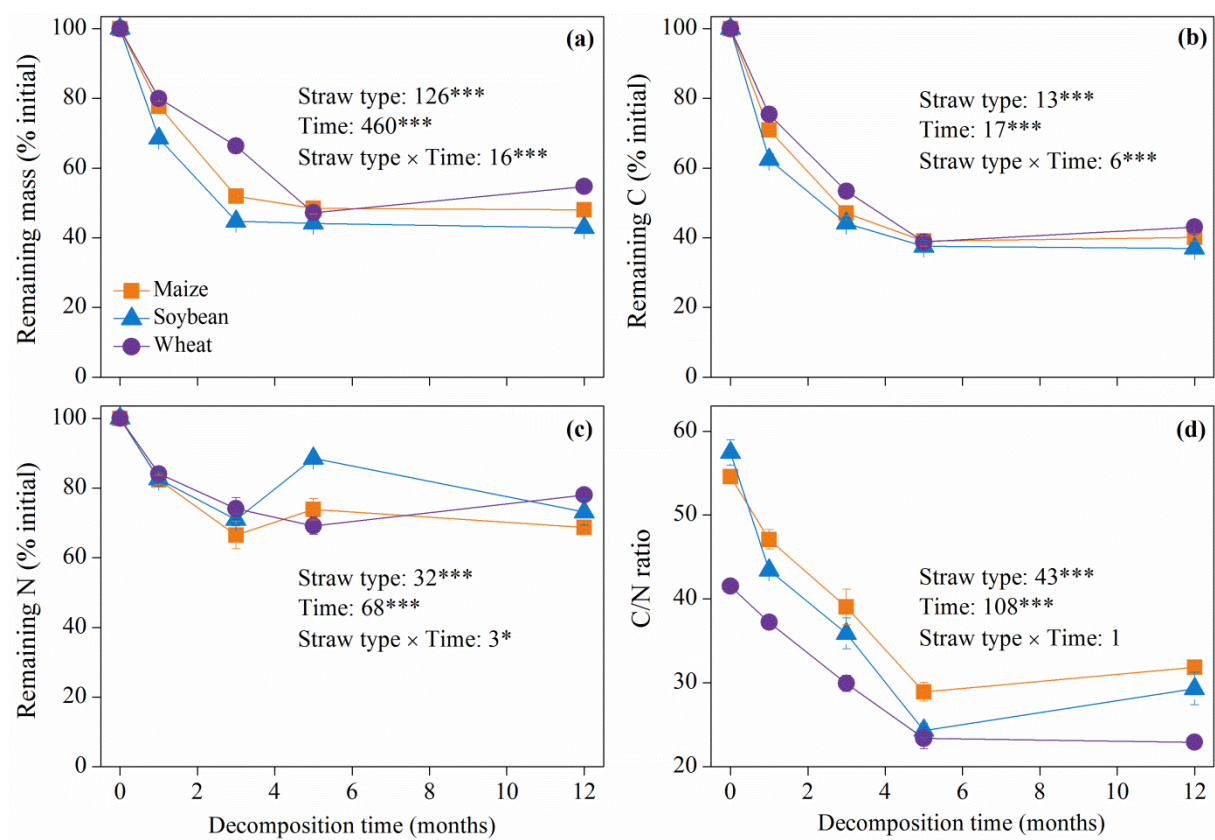
829

830 **Fig. 6.** Annual **(a)** soil organic carbon (SOC) sequestration and **(b)** nitrogen (N) supply by  
831 returning maize, soybean, or wheat **residues** to soil with full amount. Vertical bars are the  
832 standard errors ( $n = 4$ ). Significant differences between residues at  $P < 0.05$  are indicated by  
833 different lowercase letters. **It should be noted that this is a litterbag study so N supply and**  
834 **SOC sequestration is probably much different from those obtained under direct soil-residue**  
835 **contact.**

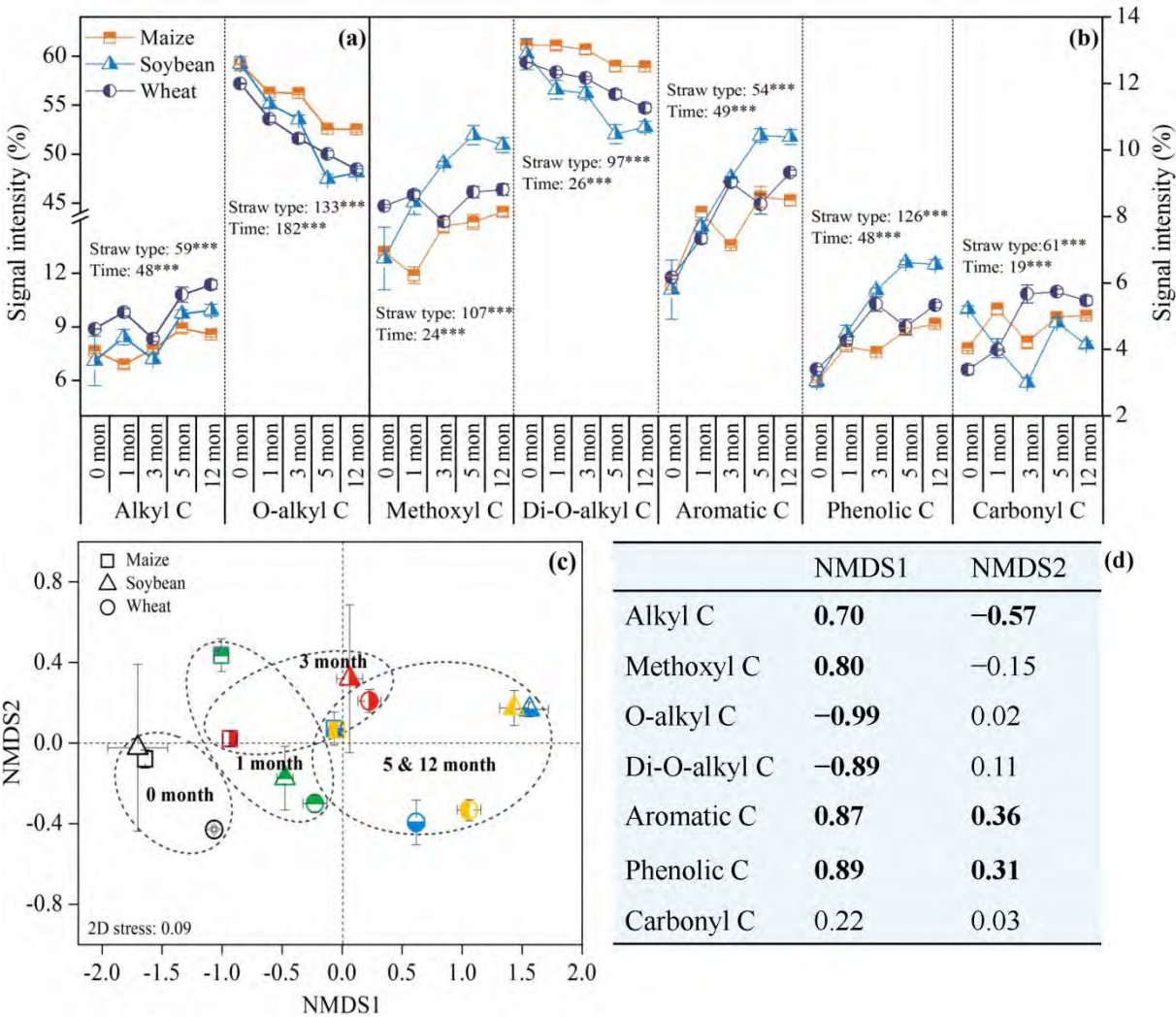
836 **Fig. 1.**



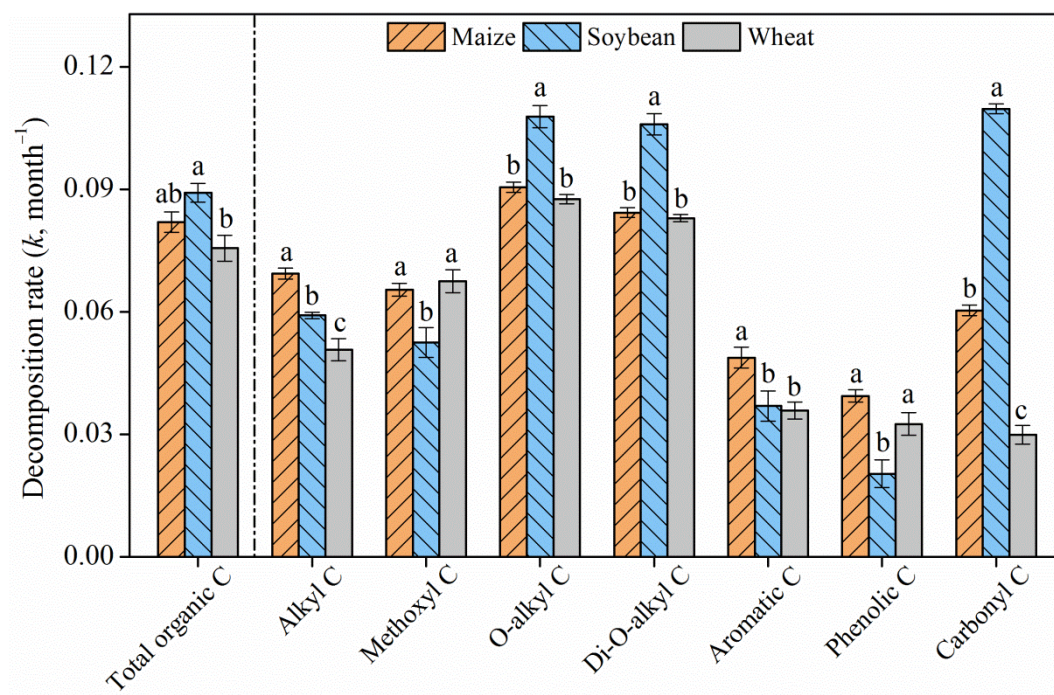
838 **Fig. 2.**



839

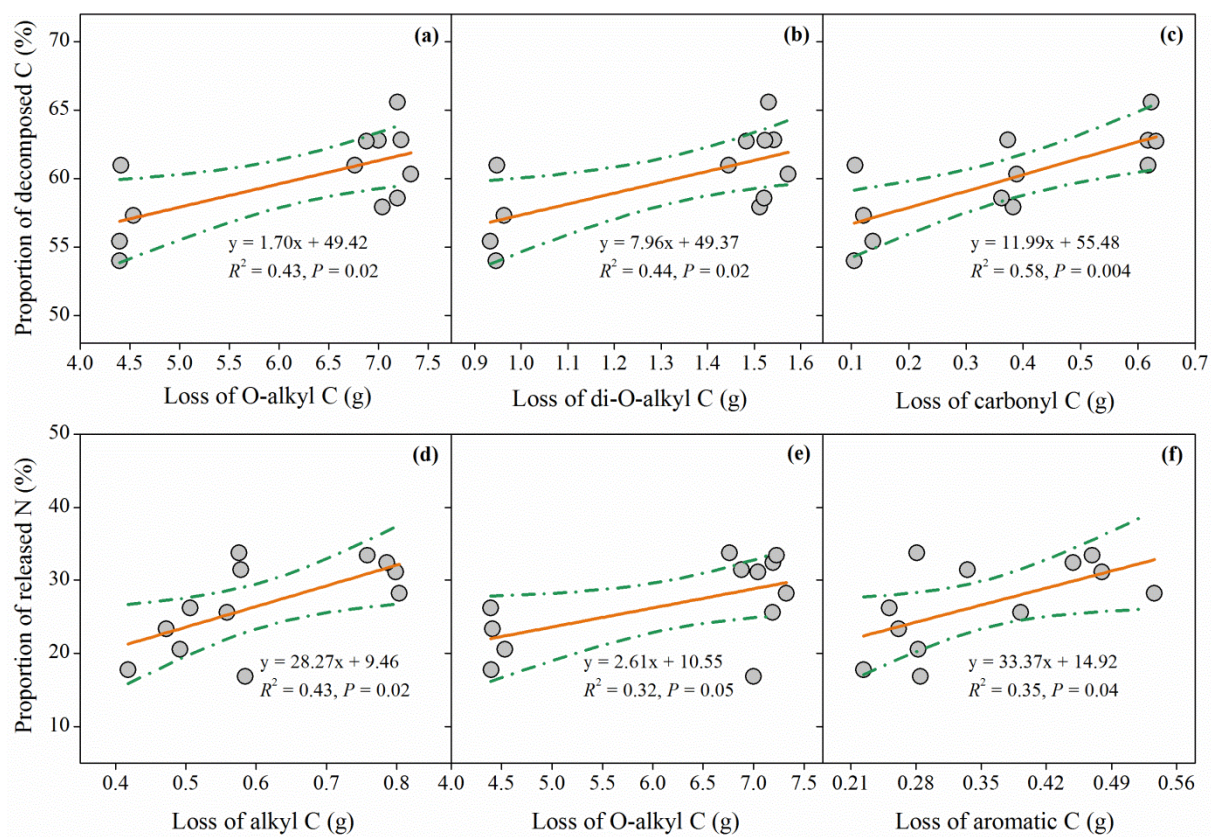


842 **Fig. 4.**



843

844 **Fig. 5.**



845

**Fig. 6.**

